J. Fluid Mech. (2010), *vol.* 642, *pp.* 279–294.
doi:10.1017/S002211200999187X

Turbulent drag reduction with polymer additive in rough pipes

SHU-QING YANG[1]† AND G. DOU[2]

[1]School of Civil, Mining & Environmental Engineering, University of Wollongong NSW 2522, Australia

[2]Nanjing Hydraulic Research Institute, 223 Guangzhou Road, Nanjing, China, 210024

(Received 17 December 2009; revised 31 August 2009; accepted 31 August 2009; first published online 11 December 2009)

Friction factor of drag-reducing flow with presence of polymers in a rough pipe has been investigated based on the eddy diffusivity model, which shows that the ratio of effective viscosity caused by polymers to kinematic viscosity of fluid should be proportional to the Reynolds number, i.e. u_*R/ν and the proportionality factor depends on polymer's type and concentration. A formula of flow resistance covering all regions from laminar, transitional and fully turbulent flows has been derived, and it is valid in hydraulically smooth, transitional and fully rough regimes. This new formula has been tested against Nikuradse and Virk's experimental data in both Newtonian and non-Newtonian fluid flows. The agreement between the measured and predicted friction factors is satisfactory, indicating that the addition of polymer into Newtonian fluid flow leads to the non-zero effective viscosity and it also thickens the viscous sublayer, subsequently the drag is reduced. The investigation shows that the effect of polymer also changes the velocity at the top of roughness elements. Both experimental data and theoretical predictions indicate that, if same polymer solution is used, the drag reduction (DR) in roughened pipes becomes smaller relative to smooth pipe flows at the same Reynolds number.

Key words: general fluid mechanics, pipe flows, polymers

1. Introduction and background

Drag reduction (DR) by polymer additives in turbulent flows was first discovered by Toms in 1948, i.e. the dilute addition of high-molecular-weight polymers to flowing liquids can drastically reduce the turbulent friction up to 80 % (Benzi *et al.* 2004*a*,*b*; L'vov *et al.* 2004). This provides a potential solution for piping and shipping industries to save energy. This intriguing phenomenon is by now well known, and intensive experimental, numerical and analytical works have been documented. Comprehensive reviews of this research have been done by Lumley (1969), Virk (1975*a*), McComb (1990), Sreenivasan & White (2000), White & Mungal (2008) and others.

While experimental data have accumulated over the past 60 years, the fundamental theory of DR due to polymer remains elusive. Recently, some progress in the model of DR has been made by Procaccia, L'vov & Benzi (2008) and L'vov *et al.* (2004). They successfully provided a quantitative explanation of the maximum drag reduction

† Email address for correspondence: shuqing@uow.edu.au

(MDR) asymptote that has the following form:

$$u^+ = 11.7 \ln y^+ - 17, \tag{1}$$

where $u^+ = u/u_*$ and $y^+ = u_* y/\nu$, and u = time-averaged velocity, u_* = shear velocity, y = distance to the wall and ν = kinematic viscosity.

Virk (1971*a*) discovered that in the turbulent core of a polymer solution the velocity follows a log law with the same slope as Newtonian fluid flow, but with some velocity increment ΔB, i.e.

$$u^+ = 2.5 \ln y^+ + 5.5 + \Delta B. \tag{2}$$

Benzi *et al.* (2004*b*) found that if the constant 5.5 is replaced with 6.13, then ΔB can be expressed by the following equation:

$$\Delta B = 9.4 \ln \left(1 + \xi^3 N_p^3 C\right), \tag{3}$$

where ξ is an effective hydrodynamics radius of monomer (depending on the chemical composition), N_p the degree of polymerization and C the polymer concentration by volume.

Using a different approach, Yang & Dou (2005, 2008) developed another model that rests on the assumption that the phenomenology of polymer DR can be described by a modified eddy diffusivity parameter. Starting from the eddy diffusivity model, they successfully simulated the velocity profiles and turbulent structures in drag-reducing flows over a smooth boundary. As the DR phenomenon is a near-wall effect, it would be useful to investigate the DR flows over a rough boundary.

For a rough pipe flow, it is well known that there exist three regions, namely laminar, transitional and fully turbulent. Experiments (Schlichting 1979, p.452) show that in the transitional region, turbulence is of intermittent nature, occurring at one moment and disappearing at another, the turbulent and the laminar states are interchangeable. Based on this, Dou expressed the velocity from laminar to turbulent flow with the following equation (Yang & Dou 2005):

$$u_t^+ = r_l u_l^+ + r_t u^+, \tag{4}$$

where u_t^+ is the relative velocity in the transition region, u_l^+ the relative velocity in laminar flow, u^+ the relative velocity in fully turbulent flow, r_l the probability of laminar occurrence, r_t the probability of turbulent occurrence and

$$r_t + r_l = 1. \tag{5}$$

Dou (1996) obtained the following equation for r_l:

$$r_l = \begin{cases} \dfrac{1}{e}\left[\displaystyle\sum_{n=1}^{\infty} \frac{n}{n!}\left(\frac{R_c^+}{R^+}\right)^{2n}\right] & R \geqslant R_c, \\ 1 & R < R_c, \end{cases} \tag{6}$$

where R^+ = Reynolds number $= u_* R/\nu$, and R = pipe radius, R_c^+ = critical Reynolds number at which the laminar flow transits to turbulent status.

Yang & Dou (2005, 2008) expressed the polymer shear stress or the 'shear deficit' in drag-reducing flow in the following form:

$$\tau - \left[\mu \frac{\mathrm{d}u}{\mathrm{d}y} + (-\rho\overline{u'v'})\right] = \rho \nu_{eff} \frac{\mathrm{d}u}{\mathrm{d}y}, \tag{7}$$

where τ = total shear stress $= \rho u_*^2 (1 - y/R)$, ρ = fluid density, μ = dynamic viscosity, $-\rho\overline{u'v'}$ = Reynolds shear stress, ν_{eff} = effective viscosity caused by polymer additives.

Using an analogy with Boussinesq's expression for the eddy viscosity in turbulence, they postulated that the effective viscosity can be modelled by

$$\nu_{eff} = \alpha_* u_* R, \tag{8}$$

where α_* is an elastic factor depending on the polymer type and concentration. Dou (1981) obtained an empirical equation for α_*

$$\alpha_* = A[\eta]C\alpha_o \exp\left(-B\alpha_o^{0.7}C_w\right), \tag{9}$$

in which A is a constant and equal to $\pi^2/15$; B is equal to 25 500; $[\eta]$ is the intrinsic viscosity of polymer; C is the concentration of solution (g cm^{-13}); C_w is the concentration of solution by weight (g g^{-1}); α_o is a coefficient which depends on polymer's characteristics for DR.

Different from (8), Procaccia *et al.* (2008) expressed the effective viscosity in the following way:

$$\nu_{eff} = \nu\xi^3 C N_p^3. \tag{10}$$

In the transitional region, the Reynolds shear stress can be expressed by

$$(-\overline{u'v'})_t = -\overline{(\gamma_t u')(\gamma_t v')} = r_t^2(-\overline{u'v'}). \tag{11}$$

Virk (1971*b*) observed that DR occurs only when the flow is in turbulent state, or $-\overline{u'v'} \neq 0$, so it is understandable that in the transitional region ν_{eff} appears when turbulence appears. In other words, the effective viscosity should be proportional to r_t^2 as the Reynolds shear stress in (11). Therefore, inserting (8) into (7), one obtains

$$u_*^2\left(1-\frac{y}{R}\right) = (\nu+\nu_{eff})\frac{\mathrm{d}u}{\mathrm{d}y} - \overline{u'v'} = \nu D_*\frac{\mathrm{d}u}{\mathrm{d}y} - \overline{u'v'}, \tag{12}$$

where D_* is the DR parameter and

$$D_* = 1 + \alpha_* r_t^2 \frac{u_* R}{\nu}. \tag{13}$$

If $-\overline{u'v'} = 0$, one can obtain the velocity u_l^+ in laminar flow from (12), and by modelling the Reynolds shear stress in (12), Dou obtained the velocity u^+ in fully turbulent flow (Yang & Dou 2008). Inserting the obtained u_l^+ and u^+ into (4), one obtains the following equation:

$$u_t^+ = r_l\frac{y^+}{D_*}\left(1-\frac{y^+}{2R^+}\right) + r_t\left[\frac{1}{\kappa}\ln\left(1+\frac{\kappa y^+}{2D_*}\right) + \frac{1}{2}\left(\frac{u_*\delta}{\nu D_*}+\frac{1}{\kappa}\right)\left(\frac{\kappa y^+}{2D_*+\kappa y^+}\right)^2 + \frac{1}{\kappa}\frac{\kappa y^+}{2D_*+\kappa y^+} + C_1\right], \tag{14}$$

where $\kappa = 0.4$, $u_*\delta/\nu = 11.6D_*^3$ and C_1 is an integration constant.

If $R^+ < R_c^+$, (5) and (6) show $r_l = 1$ and $r_t = 0$, (14) becomes the velocity profile of laminar flow. When the Reynolds number is large enough, we have $r_l = 0$ and $r_t = 1$, so (14) expresses the velocity in fully turbulent flow. It can be seen that (14) is a general formula of velocity distribution for viscoelastic fluid flow in laminar, transitional and fully turbulent regions.

In a fully turbulent flow, i.e. $r_l = 0$ and $r_t = 1$, if $\kappa y^+ \gg 2D_*$, (14) can be simplified as (2) and ΔB has the following form:

$$\Delta B = 5.8(D_*^2 - 1) - 2.5\ln D_*. \tag{15}$$

By comparing (15) with (3), one concludes that these two approaches have different expressions. Equation (3) shows that the velocity increment ΔB depends on polymer

parameters only, but (15) demonstrates that ΔB depends on D_*, a function of polymer parameters and also Reynolds number.

The eddy diffusivity model in (8) expresses the interactions of the polymers with turbulence as the shear velocity u_* represents the turbulent strength, R represents the size of the largest eddies and the influence of polymer is included in the parameter α_*. However, Benzi *et al.* (2004*a*) model only relates the polymeric viscosity to polymer concentration and its chemical composition regardless of turbulent strength, and no flow parameters like u_* and R are included in their effective viscosity. Because of this difference, (3) states that ΔB is independent of Reynolds number and (10) shows that ν_{eff} is proportional to the polymer concentration. But (15) demonstrates that ΔB is a function of Reynolds number, and the influence of polymer concentration on the DR is expressed by (8) and (9). Therefore, it is useful to justify these two models using experimental data available in the literature. A plausible theory should be tested against many aspects of DR, such as qualitative and quantitative changes in the mean velocity profile, alteration of turbulent stresses, polymer concentration and the friction factor. This study will concentrate on the DR in rough pipes.

Rough pipe flow is very common in practice and also very useful in fundamental research. A widely accepted view regarding DR due to polymer addition is that the wall plays an important role for thickening the viscous sublayer (Yang & Dou 2005, 2008) and the buffer layer (Cadot, Bonn & Douady 1998; Massah & Hanratty 1997; Min *et al.* 2003; White & Mungal 2008) because polymers stretch primarily in the near-wall region of the flow, and polymers directly interact with and dampen the quasi-streamwise vortices (Goldshtik, Zametalin & Shtern 1982). Hence, it is important to know how the polymers interact with 'rough skin' and it is needed to check the validity of (3) and (15) in rough pipes.

In practice, the prediction of pressure drop gradient and the evaluation of the drag along pipelines are of considerable industrial importance in the transport of liquids. To apply the technology of DR by polymer additives in pipelines, engineers need a reliable way to estimate the friction factor in their design, especially in rough pipes. Unfortunately, no such formula is available in the literature. In fundamental research, the friction factor in rough pipes is also of particular interest because it offers the possibility of inferring features of the wall-flow structure from relatively simple friction factor measurement (Virk 1971*a*). Thus the rough wall case is important in both practical applications and fundamental research for the underlying mechanism of DR in flows.

The friction factor is normally defined as

$$f = 2\left(\frac{u_*}{V}\right)^2, \tag{16}$$

where $f =$ friction factor and $V =$ overall average velocity.

Nikuradse (1933) systematically measured the friction factor of Newtonian fluid flow in rough pipes. His experiment shows that the friction factor depends on the Reynolds number and the relative roughness, R/Δ where Δ is Nikuradse's equivalent roughness height. If the Reynolds number is very small, the friction factor in rough pipes behaves as though it was smooth. If the Reynolds number is high enough, the friction factor is independent of Reynolds number and only relies on the relative roughness. Between these two extremes, there is a transition region where the friction factor depends on both Reynolds number and relative roughness.

Although a large number of studies have been experimentally conducted to investigate the friction factor of pipe flow with polymer additives, most of them

were carried out over a smooth surface, such as Sibilla & Baron (2002), Warholic *et al.* (2001) and Ptasinski *et al.* (2001), etc. Only a few (Lindgren & Hoot 1968; Virk 1971*a*; Bewersdorff & Thiel 1993; Wojs 1993; Petrie *et al.* 2003; Vlachogiannis & Hanratty 2004) have considered a roughened wall. Based on his experiment, Virk (1971*a*) reported that the friction factor of polymer solution in a laminar flow is the same as that in Newtonian fluid flows. But following onset, the DR induced by a given polymer solution is a complex function of flow and polymeric parameters and of pipe roughness. Till now, no equation is available to express the complex interactions.

The objectives of this investigation are (i) to examine the relationship between the Reynolds number and the effective viscosity, (ii) to develop an equation for friction factor of DR flow in rough pipes. For the first objective, (8) and (10) will be tested using experimental data in smooth pipes. For the second objective, we will extend (14) to rough pipe flows and will establish the relationship between the boundary parameter C_1 and the Reynolds number as well as the relative roughness. For the purpose of practical application, the simplified forms of these equations will be proposed and examined.

2. Influence of Reynolds number on effective viscosity

We first consider a simple case, i.e. smooth pipe flow with polymer additives. The overall averaged velocity V can be obtained from the following integration:

$$\sqrt{\frac{2}{f}} = \frac{V}{u_*} = \frac{1}{\pi R^2}\int_0^R u^+ 2\pi(R-y)\,\mathrm{d}y. \tag{17}$$

Inserting (14) into (17), one has

$$\frac{V}{u_*} = \frac{1-r_t}{4}\frac{R^+}{D_*} + r_t\left[\left(2.5 - \frac{23.2D_*^2+5}{R^+/(5D_*)} - \frac{34.8D_*^2+10}{R^{+2}/(5D_*)^2}\right)\ln\left(1+\frac{R^+}{5D_*}\right) + 5.8D_*^2 + \frac{34.8D_*^2+10}{R^+/(5D_*)} + C_1\right], \tag{18}$$

where R^+ is the Reynolds number $= u_* R/\nu$. Obviously, for smooth pipes, the non-slip boundary condition gives $u=0$ at $y=0$, then (14) gives $C_1 = 0$.

Equation (18) may be too cumbersome for an ordinary engineer in their pipeline design, therefore it would be useful to simplify it. Empirically, (18) can be simplified as follows:

$$\frac{V}{u_*} = \frac{1-r_t}{4}\frac{R^+}{D_*} + r_t\left(2.5\ln\frac{R^+}{D_*} - 66.69\left(\frac{R^+}{D_*^{3.5}}\right)^{-0.72} + 5.8D_*^2 - 4\right). \tag{19}$$

Calculation shows that the relative discrepancy between (18) and (19) is less than 3 %, indicating that (19) is also suitable for practical application.

For Newtonian fluid flow, experiments show that for a circular pipe the critical Reynolds number $Re_c = VD/\nu$ is about 2300 (Keefe, Moin & Kim 1992; Matas, Morris & Guazzelli 2003), where D is the diameter of pipe. Escudier & Smith (1999) observed that R_c^+ is affected by the presence of polymer, but Draad, Kuiken & Nieuwstadt (1998) reported that the large body of available literature on DR shows no change in the critical Reynolds number, and the transition to turbulence for drag-reducing flow occurs at the same value as for Newtonian fluids, i.e. $Re_c = 2300$.

In laminar status, $r_t = 0$, and (13) gives $D_* = 1$. Inserting these two values into (18), one obtains

$$\frac{Re}{2R^+} = \frac{1}{4}R^+. \tag{20}$$

Therefore, the critical Reynolds number can be obtained by $R_c^+ = (2Re_c)^{0.5} = (2 \times 2300)^{0.5} = 67.82$. This critical Reynolds number is valid for both Newtonian fluid and polymer solution, as well as smooth/rough pipes (Virk 1971*a*). This study assumes that R_c^+ is independent of polymer type and concentration in order to simplify the expression.

In the transition region, for any given Reynolds number R^+ one can calculate r_t based on (5) and (6), then D_* can be determined using (9) and (13) if polymer concentration, intrinsic viscosity of polymer and α_o are provided. The intrinsic viscosity (in $\mathrm{cm}^3\ \mathrm{g}^{-1}$) can be assessed using the molecular weight of polymer M (Mun, Byars & Boger 1998) by

$$[\eta] = 1.03 \times 10^{-3} M^{0.78}. \tag{21}$$

If (18) is used to predict the friction factor, there is a single unknown to determine, i.e. α_o that only depends on the type of polymer used and is independent of polymer concentration. Therefore the first step to apply (18) is to calibrate α_o using experimental data, after the calibration (18) can be used to predict the friction factor at any Reynolds number (R^+) and any concentration (C) of the polymer.

Benzi *et al.* (2004*a*) used Virk's three-layer model (Virk 1971*a*), namely a viscous sublayer near the wall, a turbulent core or Newtonian plug (defined in (2)) and a logarithmic elastic sublayer (defined in (1)) between the turbulent core and viscous sublayer. The overall averaged velocity V can be determined from the following equation:

$$\frac{V}{u_*} = \frac{1}{\pi R^{+2}}\left[\lim_{\varepsilon \to 0}\int_{\varepsilon}^{y_v^+} u^+ 2\pi(R^+ - y^+)\,\mathrm{d}y^+ + \int_{y_v^+}^{R^+} u^+ 2\pi(R^+ - y^+)\,\mathrm{d}y^+\right], \tag{22}$$

where y_v^+ is the location at which (1) and (2) intersect each other. Inserting (1) and (2) into the first and second terms on the right-hand side of (22), one has

$$\begin{aligned}\frac{V}{u_*} = {} & \frac{1 - r_t}{4}R^+ + r_t\left[11.7\frac{y_v^+}{R^+}\ln y_v^+\left(2 - \frac{y_v^+}{R^+}\right) - 57.4\frac{y_v^+}{R^+} + 22.85\frac{y_v^{+2}}{R^{+2}} + 2.5\ln R^+\right. \\ & \left. + 2.5\ln y_v^+\frac{y_v^+}{R^+}\left(\frac{y_v^+}{R^+} - 2\right) + 1.13 + \Delta B - (7.26 + 2\Delta B)\frac{y_v^+}{R^+} + (6.13 + \Delta B)\frac{y_v^{+2}}{R^{+2}}\right],\end{aligned} \tag{23}$$

where ΔB is expressed in (3) and

$$y_v^+ = 11.7\left(1 + \xi^3 N_p^3 C\right). \tag{24a}$$

Substituting (23) and (24*a*) into (16), one can determine the friction factor also. Although there are two unknowns to calibrate using experimental data, namely ξ and Np, they can be treated as a single unknown, i.e.

$$\alpha_1 = (\xi\, N_p)^3. \tag{24b}$$

Therefore, both Benzi *et al.* (2004*b*) model (defined in (23)) and the eddy diffusivity model (defined in (19)) contain one unknown to be calibrated using experimental data, namely α_0 and α_1. Once they are determined for a specified polymer solution, the friction factor of drag-reducing flow at different Reynolds number and concentrations

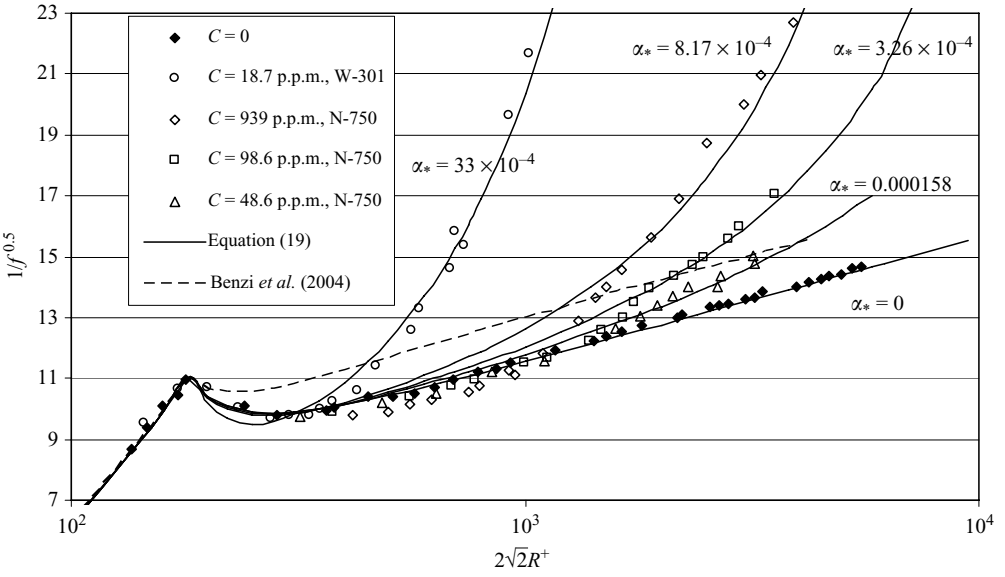

FIGURE 1. Comparison of friction factor between the eddy diffusivity model and Benzi *et al.* (2004*a*) model with Virk's experimental data in smooth pipes.

of this polymer could be predicted. It would be interesting to check the predictability of these two approaches.

Herein we use the experimental data by Virk (1971*a*) who conducted a systematic experimental measurement of friction factor of viscoelatic flow with polymer additives in circular pipes. The dilute solution of highly efficient polyethylene oxide (PEO) W-301 and ordinary PEO N-750 and pure water were used in his experiments. He reported that the intrinsic viscosity of N-750 and W-301 were 310 and 1850 $cm^3\ g^{-1}$, respectively. He measured friction factor $f = 0.00889$ in a smooth pipe flow in the presence of polymer (N-750) at concentration $C = 43.6$ p.p.m. and Reynolds number $R^+ = 1120$. He then repeated the measurement by changing the Reynolds number and polymer concentration, and the measured data are shown in figure 1.

Inserting $R^+ = 1120$ into (6), one obtains $r_l = 0$, and $r_t = 1$, indicating the flow is in fully turbulent region. Using (16), one can calculate $V/u_* = (2/0.00889)^{0.5} = 15$. From (19), one can determine the DR parameter $D_* = 1.177$. Equation (13) gives $\alpha_* = (1.177 - 1)/1120 = 1.58 \times 10^{-4}$. Based on the intrinsic viscosity, polymer concentration and the obtained α_*, one can determine the single unknown in the eddy diffusivity model α_0 using (9) and it gives $\alpha_0 = 0.019$. Then the calibrated α_0 can be used to calculate α_* for the concentrations of $C = 98.6$ p.p.m. and 939 p.p.m. for N-750. The results are shown in table 1, in which the value of α_0 for W-301 is obtained in the same way as that of N-750. Therefore, one is able to calculate the friction factor for the polymer solutions at these concentrations, and the results are shown in figure 1. It can be seen clearly that (19) agrees with Virk's experimental data very well, and for every line from very low Reynolds number to very high Reynolds number the elastic factor α_* remains constant, indicating that α_* depends on the polymer type and concentration, but is independent of the Reynolds number (Yang 2009). Figure 1 also demonstrates that the difference between Newtonian fluid flow and viscoelastic fluid relies on the elastic factor α_* and (19) is valid to express the friction factor for both Newtonian and viscoelastic fluid flows in the laminar, transition and fully turbulent regions.

Polymers	Molecular weight	$[\eta]$ cm^3 g^{-1}	C g cm^{-13}	α_0	α_* calculated from (9)
W-301	5.50×10^4	1850	18.7×10^{-4}	0.166	33.0×10^{-4}
N-750	0.57×10^4	310	939×10^{-4}	0.019	8.17×10^{-4}
N-750	0.57×10^4	310	98.9×10^{-4}	0.019	3.26×10^{-4}
N-750	0.57×10^4	310	43.6×10^{-4}	0.019	1.58×10^{-4} (calibrated)

TABLE 1. Characteristic values in Virk's experiments.

With the information of C, R^+, r_t and V/u_* listed above, from (23) and (24) one can similarly determine the single unknown $a_1 = 4$ in Benzi *et al.* (2004*a*) model. It is expected that (23) can predict the friction factor f at different Reynolds numbers and polymer concentrations as the eddy diffusivity model does. But the results show that their model is unable to capture the features of friction factor in drag-reducing flow, where the dashed line in figure 1 is the typical results of the model's prediction for N-750 at $C = 43.6$ p.p.m. As discussed, the main reason is that in the model of Benzi *et al.*, it is assumed that the effective viscosity depends on the polymer type and concentration only, and is independent of the strength of turbulence.

3. Flow separation behind roughness elements

From Nikuradse's experiments (Nikuradse 1933), researchers find that the friction factor in a rough pipe is different from that in a smooth pipe, and there are hydraulically smooth, transition and rough regions. In the hydraulically smooth region, the friction factor depends on the Reynolds number only; in the transition region the friction factor depends on both Reynolds number and roughness height; and in the rough region, the friction factor depends on roughness height only. In the literature, there is no widely accepted explanation for the observed results. Dou (1996) attributes the occurrence of these three regions to flow separation behind the roughness elements.

The flow near a smooth boundary is particularly simple, because the static pressure remains constant in the whole field of flow, no separation takes place and no backflow occurs. The most important feature of roughness elements is the flow separation that has been widely reported (e.g. Dou & Yang 1989; Dou 1996; Yang, Tan & Lim 2005; Yang & Tan 2008).

The flow separation behind a roughness element is similar to a falling sphere in still water where if the Reynolds number is less than 1, no separation flow is observed. As the Reynolds number increases, separation and eddies begin to form, enlarging into a fully developed wake near a Reynolds number of 1000, the equilibrium of the standing eddies is maintained when the flow is fully separated (Daughterty *et al.* 1985, p. 317). Experiments (Street, Watters & Vennard 1996, p. 501) have shown the separation point to be dependent of the Reynolds number, but if the Reynolds number is high enough, the separation is independent of the Reynolds number.

Similarly, it is reasonable to assume that there is no flow separation or eddies behind the roughness elements if the Re is very small, and separation occurs when the Reynolds number exceeds a certain value, and full separation is formed if the Reynolds number is high enough as shown in figure 2.

To explain the existence of hydraulically smooth, transitional and fully rough regions in Nikuradse's experiment, Dou (1996) proposed the linkage between the separation flow shown in figure 2 and the flow regions. Similar to the separation flow

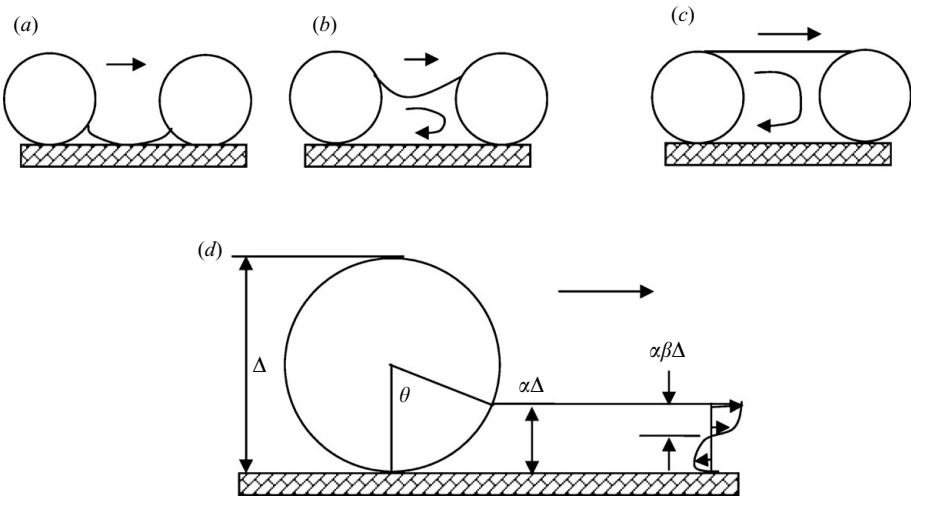

FIGURE 2. flow separation between roughness elements in different stages (*a*) hydraulically smooth, (*b*) transition, (*c*) fully rough region and (*d*) simplified flow pattern in the separation zone.

caused by a falling particle, in figure 2(*a*) if the roughness Reynolds number is very small ($u_*\Delta/\nu \approx 1.25$), we assume no eddies behind the roughness elements, or no separation occurs, in such case the roughness does not affect the turbulent structure, and rough pipe and smooth pipe perform alike.

It is understandable that if the Reynolds number ($u_*\Delta/\nu$) is higher than a certain value, say 1.25, separation flow behind roughness elements can be observed as shown in (figures 2*b* and 2*d*). As the thickness of separation layer increases with the increase of Reynolds number, one can conclude that the separation layer depends on both the Reynolds number and the roughness height. Hence, the friction factor in this region depends on both the Reynolds number and roughness height.

For very high Reynolds number ($R_* = u_*\Delta/\nu \geqslant 100$), the flow behind the roughness is fully separated or complete separation occurs (figure 2*c*) and the separation angle $\theta = 180°$. Any further increase in Reynolds number would not lead to the further increase in the separation layer, in such case the thickness of separation flow does not increase with the increase of Reynolds number, but only depends on the roughness. So the flow resistance is independent of the Reynolds number, and only dependent on the relative roughness, and consequently the flow falls in the fully rough region.

In the case of homogeneous roughness, the roughness elements can be considered approximately as spheres. If the diameter of the sphere is denoted by Δ, the separation angle by θ, and the thickness of separation by $\alpha\Delta$, we can obtain the following relation:

$$\alpha = \frac{1 - \cos\theta}{2}. \tag{25}$$

As the separation angle, θ, increases with the increase of Reynolds number and Dou (1996) assumed that the gradient $\mathrm{d}\theta/\mathrm{d}R_*$ decreases with the increase of Reynolds number, the following equation can be assumed:

$$\frac{\mathrm{d}\theta}{\mathrm{d}R_*} = \frac{a}{R_*}, \tag{26}$$

where R_* is the roughness Reynolds number ($R_* = u_*\Delta/\nu$), a is a constant proportionality to be determined. Integration of this equation yields

$$\frac{\theta}{\pi} = \frac{\ln R_* - \ln R_1}{\ln R_2 - \ln R_1}, \tag{27}$$

where R_1 and R_2 are Reynolds numbers corresponding to the initial separation and the complete separation respectively. As discussed, the experimental data by Nikuradse (1933) reveals $R_1 = 1.25$ and $R_2 = 100$.

It should be stressed that the velocity at the top of separation layer is not equal to zero, but has a definite value. The point of zero velocity locates below the separation surface because there is a region of counter current between the roughness elements as shown in figure 2(*d*).

Letting $\alpha\beta\Delta$ denote the distance from the top of separation layer to the point of zero velocity, the following assumption was made by Dou:

$$\frac{\mathrm{d}\beta}{\mathrm{d}R_*} = a_1\left[\frac{\mathrm{d}\alpha}{\mathrm{d}R_*} + \frac{\mathrm{d}(\theta/\pi)}{\mathrm{d}R_*}\right], \tag{28}$$

where a_1 is another constant of proportionality. It is obvious that when $\theta = 0$, then $\alpha = 0$ and $\beta = 1$, i.e. no counter current exists. When $\theta = \pi$, then $\alpha = 1$ and $\beta = \beta_0$. Both conditions can be used to determine the constant of integration and the constant of proportionality. Integration of (28) yields

$$\beta = 1 - \frac{(1-\beta_0)\left(\alpha + \frac{\theta}{\pi}\right)}{2}, \tag{29}$$

where $\beta = 0.107$, this value is determined from Nikuradse's data.

Considering all cases mentioned above, (27) can be rewritten as

$$\frac{\theta}{\pi} = \begin{bmatrix} 0 & \dfrac{u_*\Delta}{\nu} \leqslant 1.25 \\ \dfrac{\ln(R_*/1.25)}{\ln(100/1.25)} & 1.25 < \dfrac{u_*\Delta}{\nu} \leqslant 100 \\ 1 & \dfrac{u_*\Delta}{\nu} > 100 \end{bmatrix}. \tag{30}$$

When $R_* \geqslant 100$, complete separation occurs and the height of the separation layer does not increase with the increase of roughness Reynolds number, so that the Reynolds number should be written as follows when $R_* \geqslant 100$:

$$\frac{u_* y}{\nu} = R_*\frac{y}{\Delta} = 100\frac{y}{\Delta}, \tag{31a}$$

$$\frac{u_* R}{\nu} = R_*\frac{R}{\Delta} = 100\frac{R}{\Delta}. \tag{31b}$$

It has been pointed out that the occurrence of hydraulically smooth, transitional and rough regions is due to the degree of separation in the flow passing over the roughness elements. When $R_* > 100$, the Reynolds number is determined by (31*b*), then one can express the DR parameter D_* as follows:

$$D_{*0} = 1 + 100\alpha_* r_t^2\frac{R}{\Delta}. \tag{32}$$

Equation (32) is valid in the fully rough region where the flow is very turbulent and the thickness of the separation layer is equal to the roughness height.

4. Friction factor in rough pipe

In the case of a smooth wall, the integration constant C_1 in (14) is equal to zero. However, when the wall roughness effect is considered, the boundary condition is more complicated, and the zero velocity point is no longer at the wall ($y=0$), but shifts to a certain distance above the solid wall due to the existence of eddies behind roughness elements (see figure 2*d*). Therefore, the boundary condition for the determination of the integration constant C_1 becomes $u=u_\alpha$ at $y=\alpha\Delta$ where u_α is the mean velocity at the top of the separation layer. From (14) one has

$$C_1 = u_\alpha^+ - 2.5\ln\left(1+\frac{\alpha R_*}{5D_*}\right) - (5.8D_*^2+1.25)\left(\frac{\alpha R_*}{5D_*+\alpha R_*}\right)^2 - 2.5\frac{\alpha R_*}{5D_*+\alpha R_*}. \quad (33)$$

In the separation layer, the velocity distribution from the point where $u=0$ to the top of the separation layer can be assumed to follow (14), thus the velocity at the separation layer can be determined using the distance $\beta\alpha\Delta$, therefore the value of u_α^+ can be determined by

$$u_\alpha^+ = 2.5\ln\left(1+\alpha\beta\frac{R_*}{5D_{*0}}\right) + (5.8D_{*0}^2+1.25)\left(\frac{\alpha\beta R_*}{5D_{*0}+\alpha\beta R_*}\right)^2 + 2.5\frac{\alpha\beta R_*}{5D_{*0}+\alpha\beta R_*}. \quad (34)$$

Therefore, one can determine C_1 as follows:

$$-C_1 = 2.5\ln\left(\frac{1+\dfrac{\alpha R_*}{5D_*}}{1+\dfrac{\alpha\beta R_*}{5D_{*0}}}\right) + (5.8D_*^2+1.25)\left(\frac{\alpha R_*}{5D_*+\alpha R_*}\right)^2 + 2.5\frac{\alpha R_*}{5D_*+\alpha R_*} - (5.8D_{*0}^2+1.25)\left(\frac{\alpha\beta R_*}{5D_{*0}+\alpha\beta R_*}\right)^2 - 2.5\frac{\alpha\beta R_*}{5D_{*0}+\alpha\beta R_*}. \quad (35)$$

The values of α and β can be determined by (25) and (29) in which θ can be determined by (30). It can be seen that the integration constant in (14) can be estimated from (35). If $R_*=1.25$, one has $\theta=0$, $\alpha=0$ and $\beta=1$, and $C_1=0$, which means that the rough pipe behaves as a smooth pipe, and it is termed as the hydraulically smooth region. When $R_*>100$, as the separation angle cannot increase further the roughness Reynolds number R_* should be set as 100 in (14), (34) and (35). In such case, $\alpha=1$ and $\beta=\beta_0=0.107$, and C_1 and (18) and (19) are independent of the Reynolds number, so the friction factor is independent of the Reynolds number. For a moderate R_*, both the Reynolds number and roughness height jointly determine C_1, so the friction factor depends on these two parameters.

Inserting (35) into (18), one can obtain the formula for drag-reducing flow in rough pipes, but (35) is too complicated for an ordinate engineer, so it is useful to simplify C_1 into the following form:

$$-C_1 = \frac{D_*^{1.5}}{D_{*0}^{0.25}}\left\{\ln(R_*) + 0.325\ln\left[1+\left(\frac{R_*}{7}\right)^6\right] - 1.2\right\}. \quad (36)$$

In (36), C_1 must be negative due to the influence of roughness and polymer. Calculation shows that D_{*0} is not sensitive for the evaluation of C_1. Inserting (36)

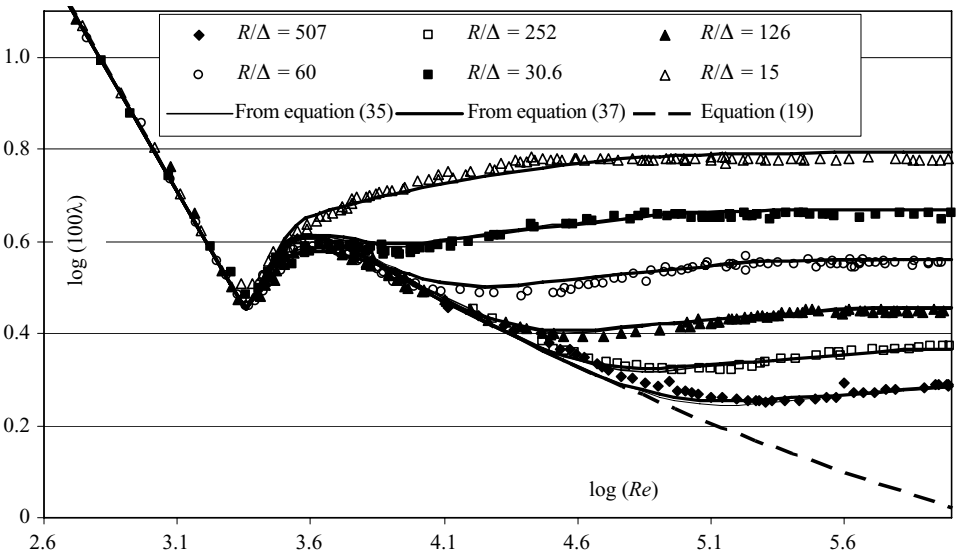

FIGURE 3. Comparison of friction factors calculated from (35) and (37) with experimental measurements from laminar to turbulent flows in rough pipes, the data points are plotted based on tables 2–7 and figure 9 of Nikurads (1933), $D_* = D_{*0} = 1$ is used in the calculation.

into (19), one has

$$\frac{V}{u_*} = \frac{1 - r_t}{4}\frac{R^+}{D_*} + r_t\left(2.5\ln\frac{R^+}{D_*} - 66.69\left(\frac{R^+}{D_*^{3.5}}\right)^{-0.72} + 5.8D_*^2 - 4 - C_1\right). \tag{37}$$

Therefore, the friction factor in a rough pipe can be obtained by substituting (35) or its simplified form i.e. (37) into (17) and (18).

In a laminar flow $r_t = 0$, and $r_l = 1$, the friction factor $\lambda[= 8(u_*/V)^2]$ can be determined using (20), i.e.

$$\lambda = \frac{64}{Re}, \tag{38}$$

where $Re = 2VR/\nu$.

In a fully developed turbulent flow, $r_l = 1$ and $r_l = 0$, if $C_1 = 0$, (18) expresses the smooth pipe flow; and if $D_* = 1$, (18) shows the mean velocity of Newtonian fluid flow. Therefore, (18) is a general expression of mean velocity which can be applied to laminar, transitional and turbulent Newtonian/viscoelastic flows including the hydraulically smooth, transitional and rough regions. It indicates that the difference between laminar/turbulent flow comes from the parameter r_t, the difference between smooth/rough pipes relies on the boundary condition C_1, and D_* expresses the difference between Newtonian fluid and viscoelastic fluid.

For verification, Nikuradse's experimental data (Nikuradse 1933) have been used in this study as shown in figure 3. It is seen that the experimental data have a 'dip' in the friction curves in the intermediate Reynolds number between fully smooth and fully rough region. To explain this phenomenon, many investigations have been conducted, but there is no consensus available in the literature to explain and quantify the dip phenomenon (Bradshaw 2000). It can be seen from figure 3 that the feature of dip phenomenon is well captured by (35), suggesting that the flow separation behind the roughness elements shown in figure 2 together with the intermittence factor provides a reasonable explanation for the observed friction factor.

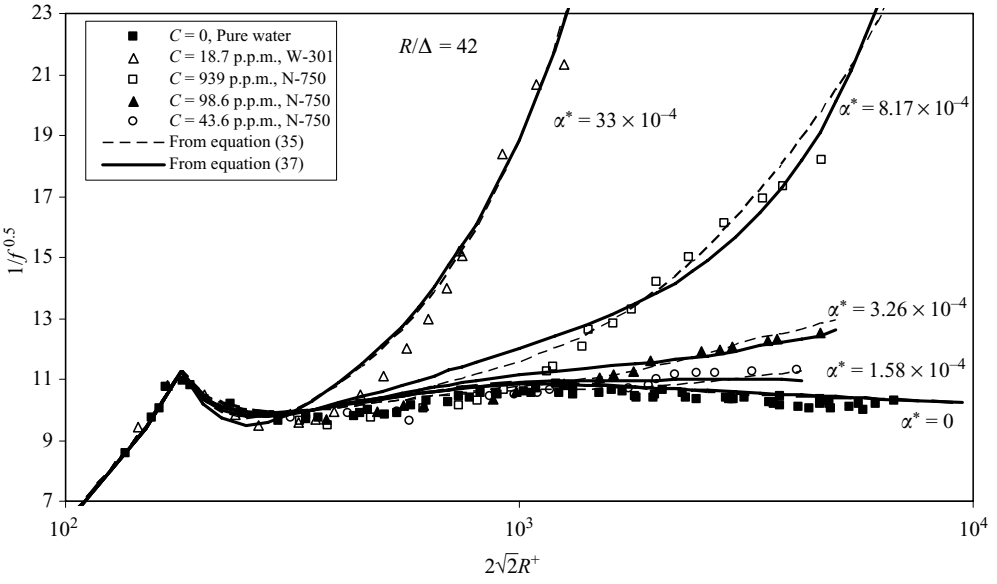

FIGURE 4. Comparison between calculated and measured friction factor in rough pipes based on Virk's experimental data

Equation (35) predicts the friction factor from very low Reynolds number (laminar flow) to very high Reynolds number (fully rough regime). To show the discrepancy between (35) and its simplified form, i.e. (37), the calculated results from (37) have also been included in figure 3 for comparison. It can be seen that there is almost no discernible difference between two of them, suggesting that (37) can be used to assess the friction factor for Newtonian fluid flow. Figure 3 also includes the prediction of (19) that gives the lower bound of friction factor in rough pipes. As shown in figure 1, (19) agrees well with Virk's experimental data.

Virk's experimental data (Virk 1971*a*) in rough pipes are used to verify (35) and (37) in viscoelastic fluid flows, and the results are shown in figures 4 and 5. After his experiments in smooth pipes, Virk carried out similar experiments in roughened pipes using different sizes of roughness. Based on the measured grit sizes, the values of R/Δ were 64.3 and 29.3, but Virk calibrated the relative roughness using distilled water resistance data and he obtained $R/\Delta = 35$ and 14.6, respectively.

When comparing the measured data in Newtonian fluid flows with (35) and (37), it is found that, different from Virk's assessment, the relative roughness R/Δ should be 42 and 16, respectively. Figures 4 and 5 show that (35) and (37) can provide satisfactory agreement with the measured data when $D_* = 1$ and $R/\Delta = 42$ and 16 are used.

Following the calibration of roughness using the experimental data in clear water flows, one can calculate the friction factors of viscoelastic fluid flows in the rough pipe. Virk measured the friction factor in the rough pipe flows where the polymer type and concentration remained the same as that used in smooth pipe flows (see figure 1). The friction factor can be predicted using (35) and (37) when R/Δ and α_* are determined, and the results are shown in figures 4 and 5. It can be seen that the experimental data cover a wide range of Reynolds numbers and include flows in laminar, transitional and turbulent states, as well as in hydraulically smooth, transitional and rough regions, the agreement between these equations and experimental data is reasonably acceptable.

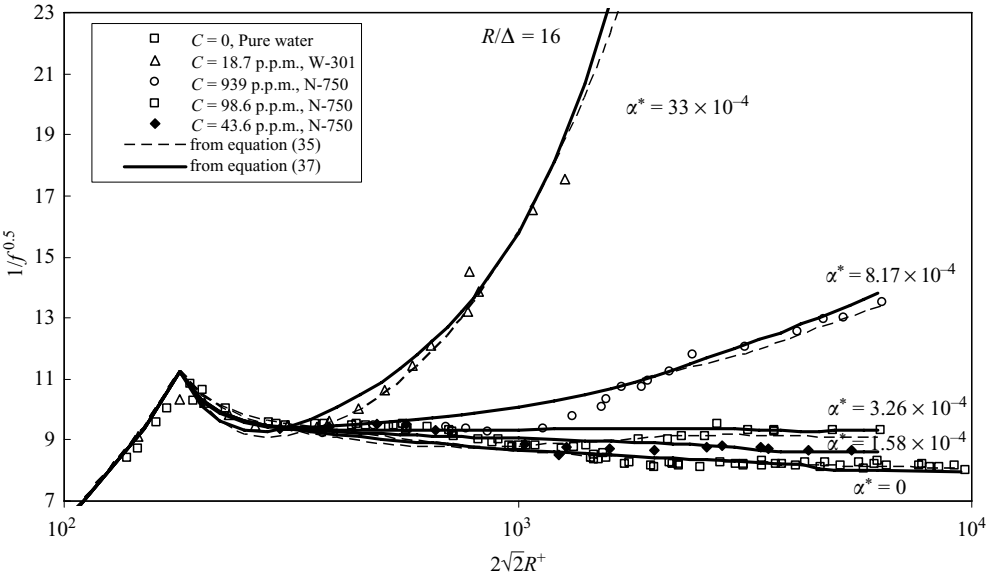

FIGURE 5. Comparison between calculated and measured friction factor in rough pipes based on Virk's experimental data

From figures 4 and 5, one may conclude that with the increase of roughness height Δ, if polymer type, concentration and Reynolds number are kept unchanged, the largest DR can be achieved in smooth pipe flow, and the efficiency of polymers for reducing the drag becomes lower in rough pipes.

It can be seen from figures 1, 4 and 5 that good agreement between the measured and predicted friction factors can be achieved when the constant effective viscosity in (8) is used, and it is determined using the data reported by Virk. It should be stressed that as the elastic factor α_* contains the influence of polymer type, its concentration or viscosity, it is expected that α_* may be variable if the polymer concentrations in the near-wall region and the main flow region are different. This means that α_* should be a function of y, which corresponds to the distribution of polymer concentration. Unfortunately, now in the literature there is no direct measurement to support this theoretical inference from (8), this leaves an open space for further experimental and theoretical investigations.

5. Conclusions

The friction factor of drag-reducing flow in the presence of polymers in a rough pipe has been investigated. A theoretical formula has been developed to describe the flow resistance in laminar, transitional and turbulent flows in hydraulically smooth, transitional and fully rough regimes. The obtained equations have been tested against the experimental data of Nikuradse and Virk, and the agreement between the measured and predicted friction factors is satisfactory. This investigation leads to the following conclusions:

(i) The effective viscosity, similar to the eddy viscosity, should be expressed as $\nu_{eff} = \alpha_* u_* R$, because the experimental data shows that the dimensionless parameter ν_{eff}/ν depends on the Reynolds number when the polymer type and concentration remain unchanged. In other words, when the polymer solution remains unchanged, the assumption of ν_{eff}/ν = constant cannot predict the curves of $f \sim Re$ as shown

in figure 1. Furthermore, it can be inferred from the eddy diffusivity model of (13) that the phenomenon of DR disappears when eddies disappear (or $r_t = 0$). This is why no DR can be observed in laminar flows.

(ii) The assumption that the hydraulically smooth, transitional and rough regions are caused by the variation of thickness of separation layer between roughness elements can yield reasonable results when compared with experimental data. The 'dip' phenomenon in Nikuradse's flow resistance curves can be well represented by the results derived from this assumption.

(iii) The investigation shows that the elastic factor α_* is independent of the relative roughness and Reynolds number. The value of the elastic factor remains constant if the polymer type and concentration are unchanged. The presence of polymer in a smooth pipe increases the thickness of the viscous sublayer, resulting in DR. In rough pipe flows, the polymer solution also increases the near-wall velocity when compared to Newtonian fluid flows, but the boundary parameter C_1 in the polymer solution is higher than its corresponding value in clear water. This means that the roughness has a negative effect on DR, or larger roughness elements tend to narrow the gap between the resistance in viscoelastic fluid flows and that in clear water flows.

(iv) In the flow of dilute macromolecular polymer solutions, from laminar flow to turbulent flow, the friction factor curves for Newtonian/viscoelastic fluids in smooth and rough pipes can be expressed by (35) or its simplified form, i.e. (37) after the turbulence occurrence probability r_t, DR parameter D_* and boundary condition C_1 are introduced.

REFERENCES

Benzi, R., Ching, E. S. C., Horesh, N. & Procaccia, I. 2004*a* Theory of concentration dependence in drag reduction by polymers and the maximum drag reduction asymptote. *Phys. Rev. Lett.* **92** (7), 078302.

Benzi, R., L'vov, V. S., Procaccia, I. & Tiberkevich, V. 2004*b* Saturation of turbulent drag reduction in dilute polymer solutions. *Europhys. Lett.* **68**, 825–831.

Bewersdorff, H. W. & Thiel, H. 1993 Turbulence structure of dilute polymer and surfactant solutions in artificially roughened pipes. *Appl. Sci. Res.* **50**, 347–368.

Bradshaw, P. 2000 A note on "Critical roughness height" and "Transitional roughness". *Phys. Fluids* **12** (6), 1611–1614.

Cadot, O., Bonn, D. & Douady, S. 1998 Turbulent drag reduction in a closed flow system: boundary layer versus bulk effects. *Phys. Fluids* **10**, 426–436.

Daugherty, R. L., Franzini, J. B. & Finnemore, E. J. 1985 *Fluid Mechanics with Engineering Applications.* McGraw-Hill.

Dou G. R. 1981 Turbulent structure in open channels and pipes. *Sci. Sin.* **24**, 727–737.

Dou G. R. 1996 Basic law in mechanics of turbulent flows. *China Ocean Engng* **10** (1), 1–44.

Dou, G. & Yang, S. Q. 1989 The drag-reducing mechanism of polymer dilute solution and its energy spectrum. *J. Nanjing Hydraul. Res. Inst.* (4), 1–12 (in Chinese).

Draad, A. A., Kuiken, G. D. C. & Niu-euwstadt, F. T. M. 1998 Laminar-turbulent transition in pipe flow for Newtonian and non-Newtonian fluids. *J. Fluid Mech.* **377**, 267–312.

Escudier, M. P. & Smith, S. 1999 Turbulent flow of Newtonian and shear-thinning liquids through a sudden axisymmetric expansion. *Exp. Fluids* **27** (5), 427–434.

Goldshtik, M. A., Zametalin, V. V. & Shtern, V. N. 1982 Simplified theory of the near wall turbulent layer of Newtonian and drag-reducing fluids. *J. Fluid Mech.* **119**, 423–441.

Keefe, L. Moin, P. & Kim, J. 1992 The dimension of attractors underlying periodic turbulent Poiseuille flow. *J. Fluid Mech.* **242**, 1–29.

L'vov, V. S., Pomyalov, A., Procaccia, I. & Tiberkevich, V. 2004 Drag reduction by polymers in wall-bounded turbulence. *Phys. Rev. Lett.* **92**, 244503.

Lindgren, E. R. & Hoot, T. G. 1968 Effects of dilute high molecular weight polymers on turbulent flows of water in very rough pipes. *ASME. J. Appl. Mech.* **35**, 417–418.

Lumley, J. L. 1969 Drag reduction by additives. *Annu. Rev. Fluid Mech.* **1**, 367–374.

Massah, H. & Hanratty, T. J. 1997 Added stresses because of the presence of FENE-P bead-spring chains in a random velocity field. *J. Fluid Mech.* **337**, 67–101.

Matas, J. P., Morris, J. F. & Guazzelli, E. 2003 Transition to turbulence in particular pipe flow. *Phys. Rev. Lett.* **90** (1), 014501.

McComb, W. 1990 *The Fluid of Physics Turbulence*. Oxford University Press.

Min, T., Yoo, J. Y., Choi, H. & Joseph, D. D. 2003 Drag reduction by polymer additives in a turbulent channel flow. *J. Fluid Mech.* **486**, 213–238.

Mun, R. P., Byars, J. A. & Boger, D. V. 1998 The effects of polymer concentration and molecular weight on the breakup of laminar capillary jets. *J. Non-Newton. Fluid Mech.* **74** (8), 285–297.

Nikuradse, J. 1933 Law of flow in rough pipes NACA TM, 1292 (English translated in 1950).

Petrie, H. L., Deutsch, S., Brungart, T. A. & Fontaine, A. A. 2003 Polymer drag reduction with surface roughness in flat-pate turbulent boundary layer flow. *Exp. Fluids* **35** (1), 8–23.

Ptasinski, P. K., Nieuwstadt, F. T. M., Van Den Brule, B. H. A. A. & Hulsen, M. A. 2001 Experiments in turbulent pipe flow with polymer additives at maximum drag reduction. *Flow Turbul. Combust.* **66**, 159–182.

Procaccia, I., L'vov, V. S. & Benzi, R. 2008 Colloquium: theory of drag reduction by polymers in wall bounded turbulence. *Rev. Mod. Phys.* **80**, 225–247

Schlichting, H. 1979 *Boundary Layer Theory*. McGraw-Hill.

Sibilla, S. & Baron, A. 2002 Polymer stress statistics in the near-wall turbulent flow of a drag-reducing solution. *Phys. Fluids* **14** (3). 1123–1136.

Sreenivasan, K. R. & White, C. M. (2000), Onset of drag reduction and the maximum drag reduction asymptote. *J. Fluid Mech.* **409**, 149–164.

Street, R. L., Watters, G. Z. & Vennard, J. K. 1996 *Elementary Fluid Mechanics*. John Wiley & Sons.

Virk, P. S. 1971*a* Drag reduction in rough pipes. *J. Fluid Mech.* **45** (2), 225–246.

Virk, P. S. 1971*b* An elastic sublayer model for drag reduction by dilute solutions of linear macromolecules. *J. Fluid. Mech.* **45**, 417–440.

Virk, P. S. 1975 Drag reduction fundamentals. *AIChE J.* **21** (4), 625–657.

Vlachogiannis, M. & Hanratty, T. J. 2004 Influence of wavy structured surfaces and large scale polymer structures on drag reduction. *Exp. Fluids* **36**, 685–700.

Warholic, M. D., Heist, D. K., Katcher, M. & Hanratty, T. J. 2001 A study with particle-image velocimetry of the influence of drag-reducing polymers on the structures of turbulence. *Exp. Fluids* **31**, 474–483.

White, C. M. & Mungal, M. G. 2008 Mechanics and prediction of turbulent drag reduction with polymer additives. *Annu. Rev. Fluid Mech.* **40**, 235–256.

Wojs, K. 1993 Laminar and turbulent flow of dilute polymer solutions in smooth and rough pipes. *J. Non-Newton. Fluid Mech.* **48**, 337–355.

Yang, S. Q. & Dou, G. 2005 Drag reduction in flat-plate turbulent boundary layer flow by polymer additive. *Phys. Fluids* **17** (6), 065104

Yang, S. Q. & Dou, G. 2008 Modelling of viscoelatic turbulent flow in open channel and pipe *Phys. Fluids* **20** (6), 065105.

Yang, S. Q. & Tan S. K. 2008 Flow resistance over mobile bed in an open-channel flow. *J. Hydraul. Engng ASCE* **134** (7), 937–947.

Yang, S. Q., Tan, S. K. & Lim, S. Y. 2005 Relation between flow resistance and bed-form geometry in wide alluvial channels. *Water Resour. Res.* **41** (9), W09419.